

Controlled Spontaneous Emission of Single Molecules in a Two-Dimensional Photonic Band Gap

Takahiro Kaji,^{*,†} Toshiki Yamada,^{*,†} Syoji Ito,[‡] Hiroshi Miyasaka,[‡] Rieko Ueda,[†] Shin-ichiro Inoue,[†] and Akira Otomo[†]

[†]Advanced ICT Research Institute, National Institute of Information and Communications Technology, 588-2 Iwaoka, Nishi-ku, Kobe 651-2492, Japan

[‡]Division of Frontier Materials Science, Graduate School of Engineering Science, and Center for Quantum Materials Science under Extreme Conditions, Osaka University, 1-3 Macikanezama-cho, Toyonaka, Osaka 560-8531, Japan

S Supporting Information

ABSTRACT: We have established a new platform to control the rate of spontaneous emission (SE) of organic molecules in the visible-light region using a combination of a two-dimensional (2D) photonic crystal (PC) slab made of TiO₂ and a single-molecule measurement method. The SE from single molecules of a perylene-3,4,9,10-tetracarboxylic diimide derivative was effectively inhibited via a radiation field controlled by the 2D PC slab, which has a photonic band gap (PBG) for transverse-electric (TE)-polarized light. The fluorescence lifetimes of the single molecules were extended up to 5.5 times (28.6 ns) by the PBG effect. This result appears to be the first demonstration of drastic lifetime elongation for single molecules due to a PBG effect.

The chemical and physical processes of electronically excited states of molecules have been applied to many photofunctional systems, such as solar energy conversion,^{1a} light-emitting diodes,^{1b} molecular data storage,^{1c} and a molecular ruler using Förster resonance energy transfer (FRET).² Because the initial process related to photofunctionality in molecular systems occurs in competition with several processes during the finite lifetime of the electronically excited state, great effort has been directed toward the acceleration of the target process to improve the functionality. From the viewpoint of the competition of various processes occurring in the excited state, control of common processes such as radiative and nonradiative transitions, and in particular a decrease in the rate constants for these transitions, can also lead to an increase in the reaction yield of the target process. Because the excited-state lifetime is generally dependent on the surrounding environment, such as the solvent or temperature, control of the lifetime of the excited state has been achieved by changes in these factors. In contrast, the application of a tailored dielectric environment via the control of the radiation field presents a greater challenge. Photonic crystals (PCs)³ can serve as tailored dielectric environments in which light propagation is altered in the periodic structure of the dielectric, thereby leading to an increase in the light–matter interaction using slow light⁴ and control of the spontaneous emission (SE) rate using a radiation field controlled by a photonic band gap (PBG)⁵ or a PC resonator.⁶ A PC resonator with a high quality factor increases the SE rate of the emitter via the Purcell effect,⁶

whereas a PBG in which the propagation of a light wave is fully restricted inhibits the SE in the PC.⁷

Although the PBG is believed to control the excited state of organic molecules by inhibiting the SE rate, thereby leading to an increase in the excited-state lifetime, clear experimental evidence has been difficult to obtain.⁸ Observing an increase in the lifetime of the excited molecules in the PBG is difficult because suppression of the emission of the ensemble molecules with inhomogeneous orientations of the transition dipoles is difficult. To suppress the emission of randomly oriented ensemble molecules within a specified frequency range, one must prepare a PC having a complete PBG⁵ that prohibits the propagation of light in all directions. However, the fabrication of a three-dimensional (3D) PC having a complete PBG in the visible-light region is difficult because of the required high level of processing accuracy.^{5c}

In contrast, a suitably designed two-dimensional (2D) PC slab could produce a PBG for transverse-electric (TE)-polarized light with an electric field confined to the *xy* plane.⁹ Therefore, the SE of a single dipole oriented in a specific direction, whose electric field is parallel to the direction of the TE polarization, can be efficiently inhibited by a 2D PC slab. In the present work, we prepared a PC slab that is transparent in the visible region ($\lambda \gtrsim 400$ nm) and has a high refractive index (RI) of 2.37 as a platform to control the SE rate of a variety of single molecules. To manufacture the oxide PC slabs, we employed a thermal annealing process that drastically reduces the background emission.¹⁰ This low background emission is important for applying the slabs to single molecules, whose fluorescence signals are weaker than those of quantum dots under the same excitation power. In addition, we adopted a single-molecule method for detecting fluorescence lifetimes.^{2,11} In ensemble measurements with a random orientation of molecules in the PBG, the portion of molecules whose SE probability is suppressed by the PBG may be too small for a difference in the fluorescence lifetimes to be detected clearly. One effective method for overcoming this difficulty utilizes fluorescence detection of single molecules because the detection of the individual molecules can provide information that is usually obscured by ensemble averaging. We experimentally obtained

Received: November 26, 2012

Published: December 19, 2012

the fluorescence properties of single molecules of a perylenediimide derivative on air-bridged PC slabs. We also studied the modification of the SE rates for single molecules depending on their orientation and position on the PC slabs.

Air-bridged TiO₂ PC slabs were prepared using electron-beam lithography and dry and wet etching processes [see the Supporting Information (SI) for details of experimental procedures]. The overall structure of the PC is illustrated schematically in Figure 1a,b. Figure 1c presents scanning

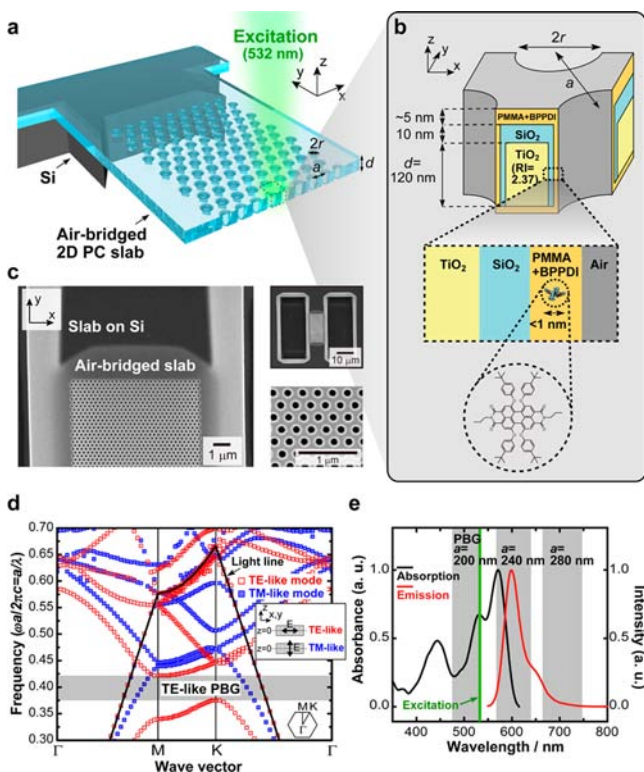


Figure 1. (a, b) Schematic diagrams and (c) SEM images of an air-bridged TiO₂ PC slab. (d) Photonic band structure of the PC slab. Red \square and blue \blacksquare indicate the TE-like and TM-like modes, respectively. (e) Absorption and fluorescence spectra of BP-PDI dye molecules. The shaded regions in (e) indicate the TE-like PBGs of PC slabs with lattice constants of 200, 240, and 280 nm.

electron microscopy (SEM) images of the PC slab. The light-gray regions in the SEM images correspond to the suspended TiO₂ membrane. The photonic band structure of the PC slab computed using a 3D finite-difference time-domain (FDTD) method (Figure 1d) indicates that a TE-like PBG is present in the normalized frequency (a/λ) range from 0.38 to 0.42, although a transverse-magnetic (TM)-like PBG is absent in all frequency ranges. Figure 1e provides the absorption and fluorescence spectra of the fluorescent dye *N,N'*-dipropyl-1,6,7,12-tetrakis(4-*tert*-butylphenoxy)-3,4:9,10-perylenetetracarboxydiimide (BP-PDI),¹² which was obtained from Yamada Chemical.^{12b} This figure indicates that the PBG overlaps the fluorescence spectrum to the greatest extent at a lattice constant (a) of 240 nm.

Figure 2a shows a confocal scanning fluorescence micrograph of the PC slab having a lattice constant of 240 nm onto which BP-PDI was coated. As shown in Figure 2a, the sides of the specimen do not have a PC structure, whereas the center is covered with the PC. We used fluorescence spot data from the

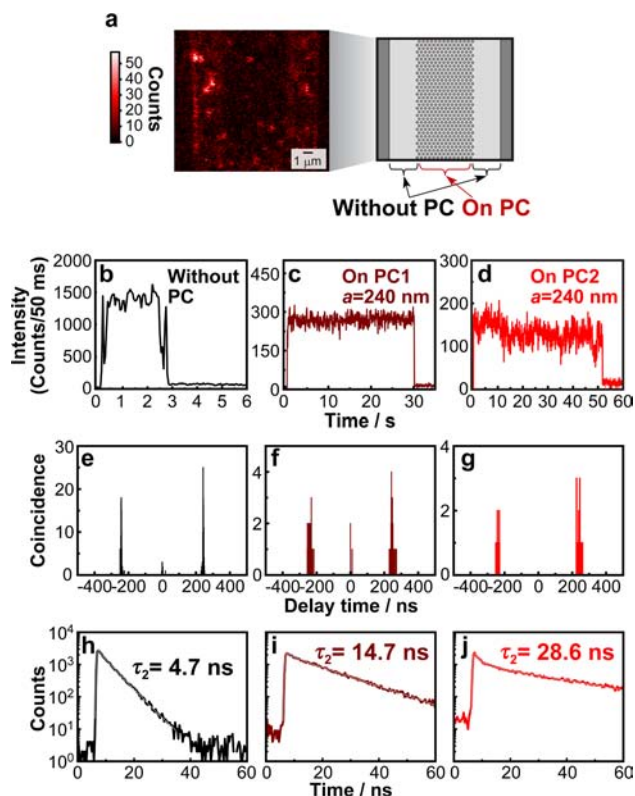


Figure 2. (a) Confocal fluorescence micrograph of a PC slab having a lattice constant of 240 nm. Representative results for (b–d) fluorescence intensity time traces, (e–g) coincidence histograms as a function of the time delay between the two detectors, and (h–j) fluorescence decay curves of (b, e, h) a single molecule without a PC and (c, f, i and d, g, j) two single molecules with a PC having a lattice constant of 240 nm.

sides of the slabs (without the PC) as a reference. Figure 2b–j provides representative results for the temporal profiles, coincidences, and fluorescence decay curves for the fluorescence spots without a PC (Figure 2b,e,h) and with a PC having a 240 nm lattice constant (Figure 2c,f,i and d,g,j). All of the fluorescence time profiles (Figure 2b–d) exhibit irreversible single-step decreases in the fluorescence intensities until the background level is reached, which strongly suggests that the fluorescence signals originate from single molecules.^{11b} To confirm detection at the single-molecule level, we plotted second-order photon correlation histograms (Figure 2e–g). The correlation values at $\tau = 0$ [$g^{(2)}(0)$] were 0.1, 0.05, and 0, respectively. These small $g^{(2)}(0)$ values clearly support the detection of single emitters.^{11a}

The fluorescence decay curves were analyzed using a biexponential function (Figure 2h–j). The decay curve without a PC (Figure 2h) was reproduced by a curve calculated using time constants of 0.8 ns (26%) and 4.7 ns (74%). In contrast, the decay curves for the PC were reproduced using time constants of 1.3 ns (25%) and 14.7 ns (75%) (Figure 2i) and 1.7 ns (63%) and 28.6 ns (37%) (Figure 2j). The longer- and shorter-lifetime components are attributed to the signals from the single molecules and the background emission from the TiO₂ slab, respectively. The lifetimes (14.7 and 28.6 ns) of BP-PDI shown in Figure 2i,j are much longer than the typical BP-PDI lifetime (~ 5 ns),¹² suggesting that the lifetimes increased dramatically as a result of the effect of the PBG.

To determine the effect of the PBG on the lifetime, the fluorescence properties of single molecules were statistically analyzed. Figure 3a,b shows the fluorescence lifetimes of BP-

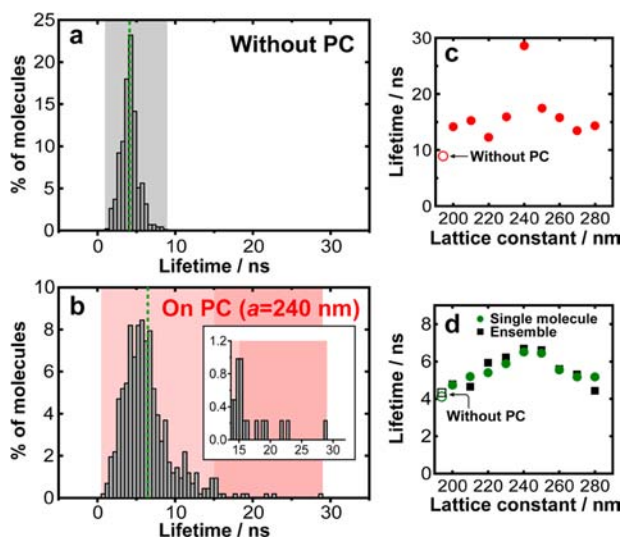


Figure 3. Distributions of fluorescence lifetimes of single molecules (a) without a PC and (b) with a PC having a lattice constant of 240 nm. Measurements of (a) 364 and (b) 400 single molecules were used to obtain the histograms. The dashed lines represent the average lifetimes. (c) Maximum lifetimes of the single molecules. (d) Average lifetimes obtained in the single-molecule (circles) and ensemble (squares) measurements. The open symbols represent the results without a PC.

PDI without a PC and with a PC having a lattice constant of 240 nm (see the SI for the results with other lattice constants). Figure 3c,d presents the maximum and average lifetimes, respectively, for each lattice constant. The range in the lifetime distributions with the PCs (Figure 3b and Figure S2b–j) is wider than that without a PC (Figure 3a), whose lifetimes are all less than 8.9 ns. At a lattice constant of 240 nm, the range of the distribution, which includes a number of molecules with longer lifetimes (15–28.6 ns), and the maximum and average lifetimes are largest. These observations strongly suggest that these longer lifetimes are due not to contamination with different chemical species but instead to elongation of the lifetimes of BP-PDI molecules through the effect of the TE-like PBG. The average lifetimes obtained from the ensemble fluorescence measurements are also provided in Figure 3d. The agreement between the lifetimes obtained through the ensemble and single-molecule measurements ensures statistical validity. In contrast, these results indicate that the single-molecule measurements detect the subpopulation of molecules with longer lifetimes that are obscured in the ensemble measurements.

The distribution of lifetimes without a PC arises from the conformational distribution and the fraction of the molecules adsorbed on the underside of the slab (without a SiO₂ layer), where lifetime shortening may occur because of photoinduced electron transfer to the TiO₂. More importantly, the distribution of BD-PDI fluorescence lifetimes on the PC can be interpreted in terms of the local modification of the SE rate for the molecules. According to Fermi's golden rule, the SE rate of an emitting dipole depends on the availability of photon modes, or the electromagnetic local density of states (LDOS).⁹ The local radiative density of states (LRDOS) accounts for the

SE rate of the dipole and is dependent on both its position and orientation. We calculated the SE rate of a dipole (see the SI for details) in three different orientations (x , y , and z) located on the surface of the slab or in an air hole (Figure 4a). Figure 4b

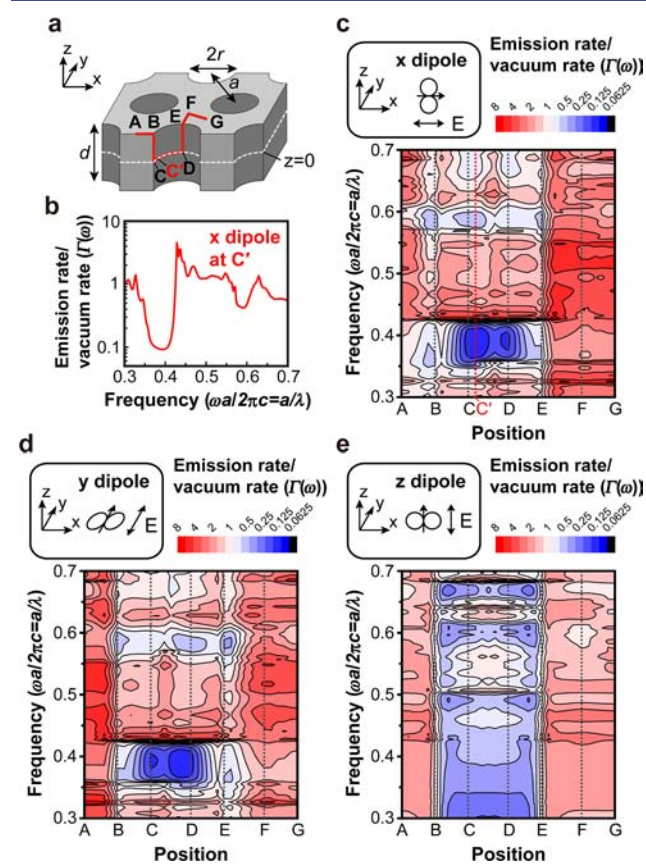


Figure 4. (a) Schematic diagram of positions A–G on a PC slab at which an emission dipole (x , y , or z orientation) was placed to calculate the SE rates. (b) SE rate relative to that in a vacuum vs the normalized frequency (a/λ) for an x dipole positioned at C' in (a). (c–e) SE rates relative to that in a vacuum for (c) x , (d) y , and (e) z dipoles at positions A–G.

shows the LRDOS normalized to that in a vacuum for an in-plane-oriented (x) dipole positioned at the plane of symmetry of the slab ($z = 0$; position C' in Figure 4a). A strong inhibition of the normalized SE rate (~ 0.1) is observed within the normalized frequency (a/λ) range 0.36–0.42. This behavior corresponds to the TE-like PBG shown in Figure 1d. Figure 4c–e summarizes the LRDOS values for the in-plane-oriented (x and y) and vertically oriented (z) dipoles located on the PC structure. For the x and y dipoles, the emission is strongly inhibited near the plane of symmetry of the slab ($z = 0$, positions C–D), whereas no strong inhibition is observed on the top surface of the slab (positions A–B, and E–G). In contrast, for the z dipole, no strong inhibition of the SE rate in the PBG region is observed at any position, as expected for structures that lack a TM-like PBG. The simulation results suggest that the molecules with long lifetimes are located near the plane of symmetry of the slab ($z = 0$; positions C–D) with an in-plane orientation.

The theoretical lifetime elongation factor of the dye (f_{sim}) was evaluated from the integrated intensities of the fluorescence spectrum in a vacuum (I_{vac}) and that modified by the PC structure (I_{PC}) using eqs 1 and 2:

$$f_{\text{sim}} = \frac{\tau_{\text{PC}}}{\tau_{\text{vac}}} = \frac{\Gamma_{\text{vac}} + k_{\text{nr}}}{\Gamma_{\text{PC}} + k_{\text{nr}}} = \frac{1}{Q_{\text{vac}} \left(\frac{1}{f_0} - 1 \right) + 1} \quad (1)$$

$$f_0 = \frac{\Gamma_{\text{vac}}}{\Gamma_{\text{PC}}} = \frac{I_{\text{vac}}}{I_{\text{PC}}} \quad (2)$$

where τ_{PC} , τ_{vac} , Γ_{PC} , and Γ_{vac} values are the fluorescence lifetimes and SE rates of the dye in the structure and in vacuum, respectively; k_{nr} is the nonradiative decay rate; and Q_{vac} is the fluorescence quantum yield in vacuum, given by $Q_{\text{vac}} = \Gamma_{\text{vac}} / (\Gamma_{\text{vac}} + k_{\text{nr}})$. The variable f_0 is the theoretical lifetime elongation factor corresponding to a fluorescence quantum yield of 1. Thus, the maximum f_{sim} for BP-PDI (x dipole at C') is 5.9 ($f_0 = 7.4$), assuming a BP-PDI quantum yield of 0.96.^{12c} In contrast, the experimental lifetime elongation factor (f_{exp}) was 5.5 on the basis of the longest lifetime ($\tau = 28.6$ ns), for which $\tau_{\text{vac}} = 5.2$ ns.^{12a} The theoretical calculation and the experimental result are in good agreement. We numerically estimated the lifetime distributions to evaluate the proportion of single molecules with longer lifetimes (see the SI for details). The lifetime distributions are shown in Figure S4b–h. These results reproduced the experimentally observed tendency of the distributions and support a small subpopulation of molecules with longer lifetimes (>15 ns) [3% for the experiment (Figure 3b), 13% for the simulation (Figure S4e)] at a lattice constant of 240 nm.

In conclusion, we have established a new photonic-crystal-based platform to control the SE rate of organic molecules by combining a 2D PC slab with a measurement at the single-molecule level. The lifetime elongation factors obtained for the single molecules (2.9–5.5) are considerably larger than those due to the effect of a PBG that have been observed for ensembles of organic molecules.⁸ This result appears to be the first demonstration of drastic lifetime elongation in single molecules due to the effect of a PBG. Our results present a new approach for controlling the excited-state lifetime and the photochemical, photophysical, and FRET processes of organic molecules via the use of a controlled radiation field. This research could also lead to the implementation of biological analysis equipment,^{4b} organic photonic devices,^{1b,4a} and molecular photonic devices^{2b} such as single-molecule lasers.

■ ASSOCIATED CONTENT

Supporting Information

Details of experimental procedures, results of the ensemble fluorescence measurements, results of the single-molecule measurements for the other lattice constants, supplemental description of the SE rate calculations, and lifetime distributions obtained by FDTD simulations. This material is available free of charge via the Internet at <http://pubs.acs.org>.

■ AUTHOR INFORMATION

Corresponding Author

kaji@nict.go.jp; toshiki@nict.go.jp

Notes

The authors declare no competing financial interest.

■ ACKNOWLEDGMENTS

This work was partially supported by Grants-in-Aid for Young Scientists (B) (22750013) and Scientific Research (C)

(24510163) from the Ministry of Education, Culture, Sports, Science, and Technology (MEXT) of Japan.

■ REFERENCES

- (1) (a) Callahan, D. M.; Munday, J. N.; Atwater, H. A. *Nano Lett.* **2012**, *12*, 214. (b) Puzzo, D. P.; Helander, M. G.; O'Brien, P. G.; Wang, Z.; Soheilnia, N.; Kherani, N.; Lu, Z.; Ozin, G. A. *Nano Lett.* **2011**, *11*, 1457. (c) Mori, K.; Ishibashi, Y.; Matsuda, H.; Ito, S.; Nagasawa, Y.; Nakagawa, H.; Uchida, K.; Yokojima, S.; Nakamura, S.; Irie, M.; Miyasaka, H. *J. Am. Chem. Soc.* **2011**, *133*, 2621.
- (2) (a) Bolinger, J. C.; Traub, M. C.; Brazard, J.; Adachi, T.; Barbara, P. F.; Bout, D. A. V. *Acc. Chem. Res.* **2012**, *45*, 1992. (b) Park, M.; Yoon, M.-C.; Yoon, Z. S.; Hori, T.; Peng, X.; Aratani, N.; Hotta, J.; Uji-i, H.; Sliwa, M.; Hofkens, J.; Osuka, A.; Kim, D. *J. Am. Chem. Soc.* **2007**, *129*, 3539.
- (3) (a) Yablonovitch, E. *Phys. Rev. Lett.* **1987**, *58*, 2059. (b) John, S. *Phys. Rev. Lett.* **1987**, *58*, 2486.
- (4) (a) Inoue, S.; Yokoyama, S. *Appl. Phys. Lett.* **2008**, *93*, No. 111110. (b) Chaudhery, V.; Huang, C.-S.; Pokhriyal, A.; Polans, J.; Cunningham, B. T. *Opt. Express* **2011**, *19*, 23327.
- (5) (a) Ho, K. M.; Chan, C. T.; Soukoulis, C. M. *Phys. Rev. Lett.* **1990**, *65*, 3152. (b) Noda, S.; Tomoda, K.; Yamamoto, N.; Chutinan, A. *Science* **2000**, *289*, 604. (c) Subramania, G.; Li, Q.; Lee, Y.-J.; Figiel, J. J.; Wang, G. T.; Fischer, A. J. *Nano Lett.* **2011**, *11*, 4591.
- (6) (a) Purcell, E. M. *Phys. Rev.* **1946**, *69*, 681. (b) Englund, D.; Fattal, D.; Waks, E.; Solomon, G.; Zhang, B.; Nakaoka, T.; Arakawa, Y.; Yamamoto, Y.; Vučković, J. *Phys. Rev. Lett.* **2005**, *95*, No. 013904.
- (7) (a) Fujita, M.; Takahashi, S.; Tanaka, Y.; Asano, T.; Noda, S. *Science* **2005**, *308*, 1296. (b) Lodahl, P.; van Driel, A. F.; Nikolaev, I. S.; Irman, A.; Overgaag, K.; Vanmaekelbergh, D.; Vos, W. L. *Nature* **2004**, *430*, 654. (c) Kounoike, K.; Yamaguchi, M.; Fujita, M.; Asano, T.; Nakanishi, J.; Noda, S. *Electron. Lett.* **2005**, *41*, 1402. (d) Kaniber, M.; Laucht, A.; Hürlimann, T.; Bichler, M.; Meyer, R.; Amann, M.-C.; Finley, J. J. *Phys. Rev. B* **2008**, *77*, No. 073312.
- (8) (a) Martorell, J.; Lawandy, N. M. *Phys. Rev. Lett.* **1990**, *65*, 1877. (b) Kolaric, B.; Baert, K.; Van der Auweraer, M.; Vallée, R. A. L.; Clays, K. *Chem. Mater.* **2007**, *19*, 5547. (c) Nikolaev, I. S.; Lodahl, P.; Vos, W. L. *J. Phys. Chem. C* **2008**, *112*, 7250. (d) Kubo, S.; Fujishima, A.; Sato, O.; Segawa, H. *J. Phys. Chem. C* **2009**, *113*, 11704. (e) González-Urbina, L.; Baert, K.; Kolaric, B.; Pérez-Moreno, J.; Clays, K. *Chem. Rev.* **2012**, *112*, 2268.
- (9) (a) Hwang, J.-K.; Ryu, H.-Y.; Lee, Y.-H. *Phys. Rev. B* **1999**, *60*, 4688. (b) Koenderink, A. F.; Kafesaki, M.; Soukoulis, C. M.; Sandoghdar, V. *J. Opt. Soc. Am. B* **2006**, *23*, 1196. (c) Sprik, R.; van Tiggelen, B. A.; Lagendijk, A. *Europhys. Lett.* **1996**, *35*, 265.
- (10) (a) Kaji, T.; Yamada, T.; Ueda, R.; Otomo, A. *J. Phys. Chem. Lett.* **2011**, *2*, 1651. (b) Kaji, T.; Yamada, T.; Ueda, R.; Xu, X.; Otomo, A. *Opt. Express* **2011**, *19*, 1422.
- (11) (a) Lounis, B.; Moerner, W. E. *Nature* **2000**, *407*, 491. (b) Hofkens, J.; Maus, M.; Gensch, T.; Vosch, T.; Cotlet, M.; Köhn, F.; Herrmann, A.; Müllen, K.; De Schryver, F. C. *J. Am. Chem. Soc.* **2000**, *122*, 9278.
- (12) (a) Vosch, T.; Fron, E.; Hotta, J.-i.; Deres, A.; Uji-i, H.; Idrissi, A.; Yang, J.; Kim, D.; Puhl, L.; Haeuseler, A.; Müllen, K.; De Schryver, F. C.; Sliwa, M.; Hofkens, J. *J. Phys. Chem. C* **2009**, *113*, 11773. (b) Ito, S.; Fukuya, S.; Kusumi, T.; Ishibashi, Y.; Miyasaka, H.; Goto, Y.; Ikai, M.; Tani, T.; Inagaki, S. *J. Phys. Chem. C* **2009**, *113*, 11884. (c) Seybold, G.; Wagenblast, G. *Dyes Pigm.* **1989**, *11*, 303.